HHS Public Access

Author manuscript

Neurobiol Dis. Author manuscript; available in PMC 2019 January 01.

Published in final edited form as:

Neurobiol Dis. 2018 January ; 109(Pt A): 1–10. doi:10.1016/j.nbd.2017.09.007.

Chemically activated luminopsins allow optogenetic inhibition of distributed nodes in an epileptic network for non-invasive and multi-site suppression of seizure activity

Jack K. Tung[1,2], **Fu Hung Shiu**[2], **Kevin Ding**[2], and **Robert E. Gross**[1,2,*]

[1]Coulter Department of Biomedical Engineering. Georgia Institute of Technology. Atlanta, GA

[2]Department of Neurosurgery. Emory University School of Medicine. Atlanta, GA

Abstract

Although optogenetic techniques have proven to be invaluable for manipulating and understanding complex neural dynamics over the past decade, they still face practical and translational challenges in targeting networks involving multiple, large, or difficult-to-illuminate areas of the brain. We utilized inhibitory luminopsins to simultaneously inhibit multiple limbic structures of the rat brain in a hardware-independent and cell-type specific manner to suppress seizure activity in a rat model of epilepsy. In addition to elucidating mechanisms of seizure suppression never directly demonstrated before, this work also illustrates how precise multi-focal control of pathological circuits can be advantageous for the treatment of epilepsy, which may also be applicable to the treatment and understanding of other neurological disorders involving broad neural circuits.

Keywords

epilepsy; optogenetics; networks; circuits; luminopsin

Introduction

Optogenetic tools have provided scientists with an unprecedented ability to manipulate neuronal activity in a temporally and spatially precise manner that has proven to be invaluable for understanding and controlling complex neural dynamics in various animal models of neurological disease[1]. Epilepsy is one such disease in which much progress has been made in identifying the crucial cell types and structures that are involved in generating and propagating seizure activity, and many of these targets have been effectively

*Corresponding author: The Emory Clinic, 1365 Clifton Road, Suite 6200, Atlanta, GA 30322, rgross@emory.edu, Phone: 404-727-2354.

Author Contributions

J.K.T, F.H.S, R.E.G. designed experiments. J.K.T, F.H.S, K.D. conducted experiments and analyzed data. J.K.T, F.H.S, K.D., R.E.G. wrote the manuscript.

Competing interests: none

manipulated with optogenetics as a direct neuromodulatory therapy to suppress seizure activity (see reviews by Krook-Magnuson et. al[2], Paz et. al[3], and Tung et. al[4]).

Despite these promising results, there still exists a translational challenge in controlling broad circuits, multiple targets, or large structures in the brain due to the practical limitations of light delivery. Indeed, the majority of light exiting a single optical fiber is completely attenuated within ~1mm from the fiber tip due to light scattering and attenuation that occurs in the brain[5]. Although progress has been made towards developing devices that can illuminate multiple sites or larger tissue volumes (e.g. multi-fiber[6], waveguides[7], red-shifted opsins[8]), these approaches have only achieved illumination of up to 10 mm^3 and usually require external hardware or chronic implants that can make them impractical for targeting multiple structures, conducting chronic experiments, or translating these approaches into clinically viable therapies. With a greater understanding that epilepsy (amongst other neurological disorders) is indeed a disorder of broad neural networks[9–13], methods for non-invasive manipulation of network activity involving multiple and/or large brain areas are needed for developing more effective treatment interventions that are amenable to chronic *in vivo* studies and future translation.

We previously demonstrated that optogenetic inhibition of neural activity can be achieved in a hardware-independent and scalable manner with inhibitory luminopsins (iLMO)[14], optogenetic probes with their own genetically encoded light source that can be activated remotely by a chemical substrate (coelenterazine, CTZ). These optogenetic probes achieve the same cell-type specific inhibition as conventional opsins without the need for external hardware or chronic implants for light delivery. We were able to demonstrate the scalability of this approach by targeting expression to multiple structures of the brain covering an estimated volume of greater than 20 mm^3[(14)]. These probes are therefore uniquely suited to address the hardware limitations and translatability of traditional optogenetic approaches.

To evaluate the utility of inhibitory luminopsins for interrogating and manipulating circuit-level activity across multiple brain regions, we expressed the inhibitory luminopsin, iLMO2, in various limbic structures of the rat and evaluated its efficacy at suppressing seizure activity. We first demonstrated that iLMO2 is able to suppress focal epileptic discharges induced by bicuculline injection in the hippocampus of anesthetized rats. We then found that simultaneous inhibition of four different nodes in the brain including the dentate gyrus (DG) and anterior nucleus of the thalamus (ANT) had an additive effect of suppressing behavioral seizures induced by pentylenetetrazol (PTZ) compared to inhibition of the individual nodes, demonstrating the utility and need for optogenetic tools capable of multi-focal, scalable, and cell-type specific control of neural activity.

Results

iLMO2 suppresses bicuculline-induced epileptic discharges in the dorsal hippocampus of anesthetized rats

To evaluate the ability of inhibitory luminopsins to suppress seizure activity, iLMO2 was selectively expressed in principal cells of the dorsal hippocampus of rats after induction of seizures by focal injection of bicuculline methiodide (BM). Two weeks following bilateral

injection of AAV-CAMKIIa-iLMO2 into the dorsal hippocampus, rats were implanted with a 16 channel cannula-electrode for chronic recordings from CA1 and CA3 of the hippocampus and injections of CTZ, vehicle, or bicuculline directly above the virus injection site, as described previously[14]. We confirmed that CTZ was indeed reaching the principal cells around the recording electrodes by direct visualization of Hoescht dye (which has a similar molecular weight to that of CTZ) injected through the cannula (Supplementary Figure 1A). The characteristics of the induced discharges are shown in Supplementary Figure 1B.

Bicuculline-induced epileptic discharges were acutely suppressed, with a corresponding decrease in broad band (0–60 Hz) power of the local field potential (LFP), following injections of CTZ (Figure 1A, *top*). Injection of vehicle did not significantly decrease the discharge rate or power of the LFP (Figure 1A, *bottom*). These effects were specific to the activity of iLMO2 and not the presence of substrate because CTZ was previously shown to have negligible effects on membrane conductance in non-transduced cells *in vitro*[15]. On average, CTZ was able to significantly reduce the discharge rate to 68.5% ± 8.4 (mean ± SEM) of baseline compared to vehicle control (Figure 1B; p=0.001, n=8 trials per group, Student's t-test). The synchrony of CA1–CA3 discharges was also significantly reduced from baseline after CTZ injection (Figure 1A,C; p=0.043, n=8 trials each, Student's t-test), while vehicle had no effect, suggesting that inhibition of principal cell activity had disrupted synchronized propagation of epileptic activity in the hippocampus.

We then asked whether iLMO2 could delay the development of epileptic discharges in the hippocampus. CTZ or vehicle was mixed with bicuculline and injected together in another group of animals expressing iLMO2 in the dorsal hippocampus and implanted with cannula-electrodes. When the CTZ-bicuculline mixture was injected through the cannula, the time to seizure onset was significantly increased (Figure 1D; p=0.035, n=5 trials per group, Student's t-test), seizure duration was significantly decreased (Figure 1E; p=0.042, n=5 trials per group, Student's t-test), and the maximum discharge frequency was significantly decreased (Figure 1F, p=0.017, n=5 trials per group, Student's t-test) compared to vehicle mixed with bicuculline. iLMO2 was therefore able to both acutely suppress and delay the development of epileptic discharges induced by focal injection of bicuculline in the hippocampus.

Optogenetic inhibition of granule cells in the dentate gyrus (DG) with iLMO2 decreases duration of behavioral seizures induced by pentylenetetrazol

The dentate gyrus of the hippocampus is a critical node in the entorhinal-hippocampal circuitry that is thought to act as a selective pattern separation filter that dampens excitatory inputs entering the hippocampal formation[16]. The function of this 'dentate gate' is thought to be disrupted in epilepsy, allowing pathological excitation to pass through the DG and spread into other limbic structures[17]. Electrophysiological[18,19], histological[20], and functional imaging[21] studies have all demonstrated that the DG becomes highly active during generalized seizures induced by PTZ, suggesting a failure of the gate to prevent the spread of activity throughout the hippocampal formation and the rest of the limbic circuitry. We therefore hypothesized that we could prevent the spread of epileptic activity by

selectively expressing iLMO2 in granule cells of the DG (Figure 2A, B) and optogenetically inhibiting them.

Animals expressing iLMO2 in the granule cells of the DG were administered CTZ before a systemic injection of PTZ. They were subsequently monitored for behavioral seizures for 45 minutes before sacrificing them for c-fos immunoreactivity. Although CTZ was able to significantly reduce the seizure duration compared to vehicle (Figure 2D; mean reduction of 99s ± 49.84 (mean ± SEM), p=0.030, n=10 animals per treatment, Student's t-test), it did not significantly increase the latency to first twitch (Figure 2C; p=0.297, Student's t-test, n=10 animals per treatment) or severity of seizures (Figure 2E; p=0.500, n=12 pairs, Wilcoxin matched pairs test). However, animals that had received CTZ prior to PTZ injection were able to recover faster (i.e. come down from peak seizure severity more quickly) than those treated with vehicle (Figure 2F), supporting the finding that the seizure duration was reduced in animals treated with CTZ.

The level of neuronal activation in the DG was assessed by measuring the expression of c-fos, an immediate-early gene that becomes upregulated with neuronal firing[22]. CTZ treatment significantly reduced the amount of c-fos expression in DG granule cells 45 minutes following PTZ administration (Figure 3A,D; p=0.002, n=12 images per group, Mann-Whitney test) compared to vehicle treated animals (Figure 3B, C). These effects were specific to iLMO2 activation because CTZ did not significantly decrease behavioral seizures or c-fos expression in the DG compared to vehicle in control animals expressing halorhodopsin (NpHR) alone (n=6 animals per treatment group) in the granule cells of the DG (Figure 2C–F, 3D).

Optogenetic inhibition of the anterior nucleus of the thalamus (ANT) increases the latency to first twitch in addition to decreasing duration of pentylenetetrazol-induced seizures

The ANT has received much attention as an important neuromodulatory target for treating limbic seizures because electrical stimulation of this structure is effective in reducing seizures in various animal models[23,24] as well in patients with epilepsy[25–27]. Nevertheless, the mechanism(s) of this therapy is still unclear[28]. Lesional[29], electrical[23], and chemical blockade[30] of the ANT all support the notion that seizure suppression is achieved by inhibiting the activity of the ANT, but this has never been functionally demonstrated, and in other contexts the mechanism of action of deep brain stimulation is thought to be via excitation of neuronal efferents[31].

We therefore optogenetically inhibited the ANT (the anterodorsal, anteroventral, and anteromedial nuclei in the rat) with iLMO2 to see if direct inhibition of glutamatergic thalamic projection neurons, the majority of neurons found in the ANT[32], could suppress behavioral seizures induced by PTZ. iLMO2 was expressed bilaterally in the ANT and was found in putative cell bodies of glutamatergic projection neurons (Figure 4A). When CTZ was administered prior to PTZ injection, there was a significant increase in the latency to first twitch (Figure 4B; p=0.025, CTZ group n=4 animals, vehicle group n=6 animals, Student's t-test) and a significant decrease in seizure duration (Figure 4C; p=0.045, n=5 animals per group, Student's t-test) compared to vehicle control. However, there was no decrease in overall seizure severity by CTZ treatment (Figure 4D; p=0.135, n=5 pairs,

Wilcoxin matched pairs test). The average Racine scores over time from PTZ administration (Figure 4F) supports the finding that CTZ treated animals had a later seizure onset and reduced seizure duration because these animals reached their peak seizure intensity later and recovered faster, respectively, compared to vehicle treated animals. The significant decrease of c-fos expression in the DG (Figure 4E; $p<0.001$, $n=16$ images per group, Mann-Whitney test) suggests that inhibition of the ANT was able to indirectly decrease the activity in the DG of the hippocampus.

Simultaneous optogenetic inhibition of the ANT and DG has an additive effect on suppressing behavioral seizures induced by pentylenetetrazol

Although inhibition of the ANT or DG was able to suppress the duration of seizures and/or delay their onset, the inability of either approach to reduce the severity of seizures prompted us to investigate a combinatorial approach to target multiple nodes in the limbic circuitry. Although the DG and ANT have been extensively studied individually, they have never been simultaneously targeted with any means of neuromodulation.

We therefore expressed iLMO2 bilaterally in both the ANT and DG to see if optogenetic inhibition on a network scale could potentially have an additive effect on behavioral seizures. When iLMO2 was expressed in both ANT and DG, seizure duration was significantly reduced in CTZ treated animals compared to vehicle (Figure 5A; $p=0.010$, CTZ group $n=5$ animals, vehicle group $n=4$ animals, Student's t-test). In contrast to groups expressing iLMO2 in either target alone, overall seizure severity was also significantly reduced (Figure 5B; $p=0.029$, $n=6$ pairs, Wilcoxin matched pairs test) in CTZ treated animals compared to vehicle. Simultaneous optogenetic inhibition of the DG and ANT therefore had a greater effect at suppressing behavioral seizures compared to inhibition of either structure alone. The average Racine scores over time after PTZ administration demonstrate that CTZ treated animals always had markedly less severe seizures over time on average than vehicle treated animals (Figure 5D). Bilateral optogenetic inhibition of both the ANT and DG with iLMO2 therefore had additive effects of suppressing generalized seizures from PTZ. C-fos in the DG of animals treated with CTZ was reduced compared to those treated with vehicle (Figure 5C; $p<0.0001$, $n=19$ images for CTZ group, $n=16$ images for vehicle group, Mann-Whitney test), which suggests that the activity of the DG was similarly suppressed during seizures.

To directly compare the combinatory effect of simultaneously inhibiting the DG and ANT with the effect of inhibiting either the DG or ANT alone, we looked at the distribution of Racine scores for each group. Among the animals that had received CTZ treatment, there was a significantly greater percentage of animals showing the mildest seizures (i.e. Racine score 1) in animals expressing iLMO2 in both the DG and ANT (DG+ANT group) compared to animals expressing iLMO2 in the DG alone ($p=0.015$, $n=10$ animals for DG group, $n=7$ animals for DG+ANT group Fisher's exact test). In addition, there was a significantly lower percentage of animals showing the most severe seizures (i.e. Racine score 4) in animals expressing iLMO2 in both the DG and ANT compared to the DG alone ($p=0.013$, $n=10$ animals for DG group, $n=7$ animals for DG+ANT group, Fisher's exact test) (Figure 5E). These effects were not observed among the vehicle treated animals (Figure 5F).

These results therefore suggest that simultaneous inhibition of the DG and ANT had an additive effect on seizure suppression.

Discussion

To the best of our knowledge, simultaneous cell-type specific manipulation of neural activity (either with optogenetic or chemogenetic methods) in multiple structures of the brain has not been previously described. We utilized the unique advantages of luminopsins to illustrate how cell-type specific optogenetic manipulation of epileptic networks can be achieved in a hardware-independent fashion, which allowed us to interrogate mechanisms of seizure suppression and explore new approaches for treating epilepsy. We first demonstrated that iLMO2 could be utilized to both acutely suppress and delay focal epileptic discharges in the hippocampus of rats. We then demonstrated that expression of inhibitory luminopsins can be scaled to multiple limbic structures and simultaneously activated to modulate behavioral seizures involving broad neural circuits. Selective inhibition of granule cells in the DG resulted in a significant decrease in seizure duration while inhibition of the ANT was able to significantly reduce both the latency to first twitch and seizure duration. Reduction of seizure severity could only be achieved with simultaneous inhibition of the ANT and DG, illustrating the utility of cell-type specific network modulation.

Although optogenetic inhibition of the hippocampus has been previously utilized to suppress bicuculline-induced discharges in the mouse, the effects were rather modest (illumination with 593nm light through a fiber optic resulted in a mean reduction of discharges by 17%)[33]. Here, we demonstrated that iLMO2-mediated inhibition of the hippocampus was able to acutely suppress epileptic discharges by 31.5% on average. We were most likely able to achieve a higher degree of suppression compared to the fiber-based illumination method used previously because we were able to influence a larger volume of tissue, which was determined by the extent of iLMO2 expression rather than by light transmittance of an optical fiber. Indeed, it was estimated that only ~0.7mm^3 of tissue around the fiber tip was being illuminated in the previous mouse study while our expression in the rat hippocampus covered more than 30 mm^3. This greater extent of inhibition was useful in the much larger hippocampus of the rat compared to the mouse, as it would have proven much more challenging to illuminate with a single optical fiber.

Direct evidence supporting the dentate gate hypothesis in epilepsy was recently provided when selective inhibition of granule cells in the DG with halorhodopsin was able to restore functionality of the gate and inhibit electrographic seizures by 66% in a mouse model of temporal lobe epilepsy[34]. Here, we provide additional evidence supporting the role of the dentate gyrus in seizure propagation using iLMO2 to inhibit the DG in a rat PTZ model of generalized seizures. Bilateral inhibition of the DG with iLMO2 was able to reduce the duration of behavioral seizures by 36.1% of control animals. It is important to note that in the acute PTZ model, the dentate gate is still functional because no hippocampal sclerosis or cell death occurs[35]. Nevertheless, functional imaging[21] and immunohistochemistry[20] reveal that the dentate gate eventually ‘opens’ from excessive excitatory input and becomes hyperactive during PTZ induced seizures. Our data therefore suggests that the gate can be

'strengthened' through optogenetic inhibition to prevent propagation of seizure activity throughout the hippocampal formation.

Although numerous lesional[29], electrical stimulation[23], and chemical blockade[30] studies of the ANT suggest that inhibition of the ANT leads to seizure suppression, this has never been functionally demonstrated; in fact it has been suggested that deep brain stimulation works instead by activating neuronal efferents[31]. We explored this question directly by using optogenetics to selectively inhibit glutamatergic neurons in the ANT during PTZ induced seizures. ANT inhibition delayed the onset of seizures (i.e. increased latency to first twitch) as well as shortened the duration of seizures, providing further evidence that inhibition of the ANT can result in seizure suppression. From functional imaging and lesional studies, we know that the ANT plays a critical role in the genesis of generalized seizures: it is the first area to show an increased BOLD response following PTZ injection, which is closely followed by the retrosplenial cortex and eventually the DG[21]. It is therefore not unexpected that inhibition of the ANT would delay the onset of seizures and shorten their duration. However, although inhibition of the ANT was able to indirectly decrease the amount of activity reaching the DG, it was not sufficient to completely suppress seizures or reduce their severity. This may be due to incomplete suppression of activity that ends up spreading and amplifying throughout the rest of the limbic circuitry. Although incomplete suppression may actually mitigate unwanted side effects of complete suppression (e.g. disruption of normal brain activity), development of more effective inhibitory luminopsins (e.g. those utilizing anion-channelrhodopsins for greater and longer lasting membrane hyperpolarization or those with activity-dependence) may allow greater control and versatility.

The recurrent excitatory connections in the limbic circuit of Papez are a prime example of how network-level activity plays an important role in neurological disease. The contribution of activity from multiple structures in the brain make it particularly challenging to manipulate network activity without risking losing specificity. Inhibitory luminopsins allowed us to target multiple structures in the brain on a network-scale with cell-type specificity. By inhibiting both the ANT and DG, we were able to significantly reduce the severity of PTZ-induced seizures, which was not achieved with inhibition of either structure alone. To the best of our knowledge, this is the first instance where four anatomically distinct regions of the brain were simultaneously manipulated with optogenetics in a hardware-independent manner. With the ability to manipulate network-wide circuits in a cell-type specific fashion, luminopsins are not only uniquely suited to study epilepsy, due to the fact that seizures can arise from dysfunction at the cellular level as well as circuit level[36,37], but also other disorders of network activity such as Parkinson's disease, depression, and pain.

Conventional optogenetics works on very short time-scales (milliseconds to seconds). In contrast, luminopsins can be activated on a delayed and sustained timescale (minutes to hours) in a dose-dependent manner[38], which may be more useful for neuromodulatory approaches such as the suppression of seizures. An alternative approach that has received much attention is the use of DREADDs – designer receptors exclusively activated by designer drugs. Suppression of neural activity can be achieved with a modified muscarinic receptor or kappa-opioid receptor coupled to the inhibitory G-protein G_i. While DREADDs

and luminopsins are both considered to be chemogenetic reagents, their mechanisms of action are very different (ionotropic light-gated channels/pumps for luminopsins, metabotropic G-protein coupled receptors for DREADDs), which can have important implications in the context of neuromodulation (e.g. GPCR activation can result in many different cellular effects other than changing ion conductance, whereas luminopsins alter membrane conductance directly through ATP-independent bioluminescence). DREADDs have been utilized focally in two recent studies to suppress seizure activity[39,40], but use in multiple regions has not yet been described. The relative advantages and disadvantages for each approach remains to be characterized.

In conclusion, we utilized the unique advantages of luminopsins to demonstrate how cell-type specific optogenetic modulation of epileptic networks can be achieved to interrogate mechanisms of seizure suppression and explore new therapies. We have demonstrated that inhibitory luminopsins are capable of suppressing focal epileptic activity and that they can be expressed in multiple brain regions and simultaneously activated to modulate behavioral seizures. We demonstrated the utility of cell-type specific network modulation by showing that optogenetic manipulation of multiple nodes in a circuit involved in epilepsy was more effective at suppressing behavioral seizures than manipulation of individual nodes. These results demonstrate how luminopsins offer a unique approach for scalable, multi-site optogenetic interrogation of neural networks with cellular specificity that can be valuable for investigating and treating neurological diseases affecting network-wide brain regions.

Methods

Viral vector production

AAV2/9 CAMKIIα-iLMO2 and AAV2/9 CAMKIIα-eNpHR3.0-EYFP was produced by the Emory viral vector core at a titer of 10^{12} viral genomes/mL.

Coelenterazine preparation

Coelenterazine-h was purchased from Promega and was solubilized in 20 mM β-cyclodextrin (Sigma) in PBS as described by Dr. Osamu Shimomura[41]. Frozen stock aliquots were kept at −20°C and protected from light. For behavioral experiments, CTZ was purchased from Nanolight and solubilized in their proprietary Inject-a-lume solvent immediately before use.

Animal experiments

All animals were purchased from Charles River Laboratories and were housed in the Emory animal vivarium with a 12hr light/12hr dark cycle. All procedures were conducted in accordance to approved guidelines from the Emory University Institute for Animal Care and Use Committee.

Stereotaxic viral injections

For animals implanted with a cannula-electrode, two month old (200–250 g) male Sprague-Dawley rats were anesthetized with 1.5–4% inhaled isoflurane and a craniectomy was made 3.3 mm posterior and 3.2 mm lateral to bregma. 1.8 μl of AAV2/9-CAMKIIα-iLMO2 was

stereotaxically injected at a depth of 3.1 mm ventral to pia targeting the dorsal hippocampus. For animals used for behavioral testing, 1.5 month old (180–200 g) male Sprague-Dawley rats were utilized and surgeries were done in pairs with cage-matched littermates (1 control and 1 experimental animal per pair). For expression in the DG, 1.8 μl of AAV2/9-CAMKIIα-iLMO2 was injected bilaterally 4.68 mm posterior to bregma, and 2.9 mm lateral to bregma, and 3.2 mm ventral to pia. For expression in the ANT, 1.8 μl of AAV2/9-CAMKIIα-iLMO2 was injected bilaterally 1.6 mm posterior to bregma, 1.4 mm lateral to bregma, and 5.5 mm ventral to pia.

Virus was injected through a glass-pulled pipette using a Nanoject injector (Drummond Scientific) at a rate of 275 nl/min and allowed to equilibrate for 5 minutes in the brain before and after each injection. After viral injections were completed, the scalp was stapled closed and animals were allowed to recover for up to two weeks.

In vivo electrophysiology

Animals were implanted with a cannula-electrode two weeks after the viral injection as described previously[14]. Briefly, a guide cannula (Plastics One) was glued to a 16-channel microwire array (Tucker Davis Technologies) so that an injection cannula could be inserted into the guide cannula and be positioned 2–3 mm from the electrode tips. Four skull screws and one cerebellar reference screw were implanted into each animal. A craniotomy was then made over the dorsal hippocampus (array angled 50° from midline and centered 3.5 mm posterior and 2.9 mm lateral to bregma) and the cannula-electrode was manually driven into the brain while continuously recording to ensure correct placement of electrodes. Electrophysiologic recordings were sampled at 25 kHz using our custom built NeuroRighter data acquisition system[42]. LFPs were bandpass filtered (1–500 Hz) from the raw signal and visualized in real-time. The entire cannula-electrode was then sealed in place with dental acrylic (Lang Dental), the optical fiber was retracted from the guide cannula and replaced with a dummy cannula, and the animal was allowed to recover several days before further experimentation.

Intracerebral injections

Intracerebral injections of CTZ and bicuculline were conducted through the cannula-electrode as described previously[14]. The chronically implanted cannula-electrode allowed for multiple trials to be conducted for each animal. For evaluating acute suppression of bicuculline induced discharges, each trial consisted of a 1 μl injection of bicuculline (1mg/mL) followed by a subsequent injection of either 1 μl of CTZ (600 μM) or vehicle (20 mM β-cyclodextrin in PBS) after a steady discharge rate of ~2 Hz was reached. For evaluating the effect of iLMO2 on the development of bicuculline induced discharges, a different group of animals underwent multiple injection trials consisting of 1 μl of a bicuculline/CTZ mixture (1 mg/mL bicuculline and 600 μM CTZ final concentration) or bicuculline/vehicle mixture (1 mg/mL bicuculline, 20 mM β-cyclodextrin in PBS final concentration). For both groups of animals, CTZ and vehicle injection trials were given in alternating order on one particular day. The animals were first lightly anesthetized by 0.5–1.5% inhaled isoflurane and a baseline recording of at least 10 minutes was recorded before

CTZ or vehicle was injected (over a period of ~5 minutes) with a Hamilton syringe connected to an injection cannula by tubing.

Behavior experiments

Animals were habituated in a tail vein restrainer (Braintree, Inc.) daily for 7 days prior to the PTZ experiment day in order to normalize stress levels during tail vein injection. On the day of the experiment, animals were placed in the restrainer and given an intravenous tail vein injection of CTZ (1 mg in 200 μl vehicle) or vehicle alone. After 5 minutes the animals were given an intraperitoneal injection of PTZ (60 mg/kg). The animals were then returned to their home cage and video recorded for up to 45 minutes before they were immediately sacrificed for c-fos immunohistochemistry.

Seizures were scored by a blinded viewer according to the modified Racine's scale: 1 – freezing/head bobbing, 2 – myoclonic jerks or isolated twitches, 3 – clonic seizures with repetitive forelimb movements, 4 – clonic/tonic seizures w/rearing and falling and loss of consciousness, 5 – status epilepticus and/or death.

Histology

After all experiments were completed, animals were sacrificed by intraperitoneal injection of Euthasol (Virbac) and transcardially perfused with 4% paraformaldehyde (PF). The heads of animals implanted with the cannula-electrodes were decapitated and kept in PF at 4°C overnight to allow for visualization of the electrode tracks. Otherwise, the brains were dissected out and allowed to fix in PF for 1 hr. After fixation, the brains were cryoprotected in 30% sucrose before coronal sections were cut on the microtome. 10 μm thickness sections were collected onto gelatin coated glass slides for c-fos immunohistochemistry. Sections were stained with primary rabbit antibody (sc-52, Santa Cruz) overnight at 4°C and anti-rabbit secondary for 1 hour at room temperature before imaging on an upright fluorescence microscope using NIS-elements acquisition software (Nikon). C-fos expression levels in all animal groups were quantified only in the DG of coronal sections located 4.6 mm posterior to bregma (the DG virus injection site) manually in ImageJ in a blinded fashion.

Data analysis and statistical methods

LFP recordings were analyzed offline using custom Matlab scripts and the Chronux toolbox[43]. Bicuculline-induced discharges were identified using amplitude and frequency thresholding scripts kindly provided by Dr. Daniel Wagenaar. CA1–CA3 synchrony between a pair of electrodes was calculated using matlab scripts from Quiroga et. al[44]. Power spectra of the LFP were obtained using the Chronux toolbox, in which the average low frequency power (0–10Hz) was thresholded (8*standard deviation of baseline) in order to determine an arbitrary seizure onset and offset for seizure duration calculations. For calculation of acute suppression of bicuculline induced discharge rate, the average discharge rate 10 minutes after intracerebral injection was started was compared to the average discharge rate 10 minutes before the start of the injection. CA1–CA3 synchrony was calculated immediately before and 10 minutes after injections.

For PTZ behavior experiments, animals that died from status epilepticus were not included in the seizure duration calculations and animals that did not seize were not counted in the latency to first twitch calculations. All animals were included in the seizure severity calculations.

Unless otherwise stated, Student's t-tests were utilized to compare differences between two means. One-tailed t-tests were conducted because we were testing whether or not our interventions could decrease seizure activity. Furthermore, we were confident that there was significant evidence from the literature suggesting the predicted directionality of the effects of our experiments. For distributions that did not approximate a normal distribution (confirmed by D'Agostino and Pearson omnibus normality tests), the Mann-Whitney (for unpaired data) or Wilcoxin ranked sum test (for paired data) was utilized. Comparisons between more than one group were done with a two-way ANOVA.

Supplementary Material

Refer to Web version on PubMed Central for supplementary material.

Acknowledgments

The authors would like to thank Drs. Claire-Anne Gutekunst, Ken Berglund, Shan Ping Yu, and Ling Wei for their helpful feedback and guidance. Special thanks to the Emory viral vector core and the rest of the Gross lab for their technical support. Funding: NS079268 and NS079757 to R.E.G., NS086433 to J.K.T.

References

1. Tye KM, Deisseroth K. Optogenetic investigation of neural circuits underlying brain disease in animal models. Nat Rev Neurosci. 2012; 13:251–66. [PubMed: 22430017]
2. Krook-Magnuson E, Soltesz I. Beyond the hammer and the scalpel: selective circuit control for the epilepsies. Nat Neurosci. 2015; 18:331–338. [PubMed: 25710834]
3. Paz JT, Huguenard JR. Optogenetics and Epilepsy: Past, Present and Future. Epilepsy Curr. 2015; 15:34–38. [PubMed: 25678887]
4. Tung JK, Berglund K, Gross RE. Optogenetic Approaches for Controlling Seizure Activity. Brain Stimul. 2016; doi: 10.1016/j.brs.2016.06.055
5. Yizhar O, Fenno LE, Davidson TJ, Mogri M, Deisseroth K. Optogenetics in neural systems. Neuron. 2011; 71:9–34. [PubMed: 21745635]
6. Bernstein JG, Boyden ES. Optogenetic tools for analyzing the neural circuits of behavior. Trends Cogn Sci. 2011; 15:592–600. [PubMed: 22055387]
7. Shim E, Chen Y, Masmanidis S, Li M. Multisite silicon neural probes with integrated silicon nitride waveguides and gratings for optogenetic applications. Sci Rep. 2016; 6:22693. [PubMed: 26941111]
8. Chuong AS, et al. Noninvasive optical inhibition with a red-shifted microbial rhodopsin. Nat Neurosci. 2014; doi: 10.1038/nn.3752
9. Gloor P. Generalized Cortico-Reticular Epilepsies Some Considerations on the Pathophysiology of Generalized Bilaterally Synchronous Spike and Wave Discharge. Epilepsia. 1968; 9:249–263. [PubMed: 4975028]
10. Laufs H. Functional imaging of seizures and epilepsy: evolution from zones to networks. Curr Opin Neurol. 2012; 25:194–200. [PubMed: 22322414]
11. Centeno M, Carmichael DW. Network connectivity in epilepsy: Resting state fMRI and EEG-fMRI contributions. Front Neurol. Jul 5.2014

12. Holmes MD, Tucker DM. Identifying the epileptic network. Front Neurol. Jul 4.2013 :7–8. [PubMed: 23420606]
13. Stefan H, da Silva FHL. Epileptic neuronal networks: Methods of identification and clinical relevance. Front Neurol. Mar 4.2013 :1–15. [PubMed: 23355832]
14. Tung JK, Gutekunst CA, Gross RE. Inhibitory luminopsins: genetically-encoded bioluminescent opsins for versatile, scalable, and hardware-independent optogenetic inhibition. Sci Rep. 2015; 5:14366. [PubMed: 26399324]
15. Tung JK, Gutekunst CA, Gross RE. Inhibitory luminopsins: genetically-encoded bioluminescent opsins for versatile, scalable, and hardware-independent optogenetic inhibition. Sci Rep. 2015; 5:14366. [PubMed: 26399324]
16. de Almeida L, Idiart M, Lisman JE. The Input-Output Transformation of the Hippocampal Granule Cells: From Grid Cells to Place Fields. J Neurosci. 2009; 29:7504–7512. [PubMed: 19515918]
17. EWL, Stringer J, Bertram E. The dentate gyrus as a control point for seizures in the hippocampus and beyond. Epilepsy Res Suppl. 1992; 7:301–313. [PubMed: 1334669]
18. Stringer JL. Pentylenetetrazol elicits epileptiform activity in the dentate gyrus of the urethane anesthetized rat by activation of the entorhinal cortex. Brain Res. 1994; 636:221–226. [PubMed: 8012805]
19. Stringer JL. Pentylenetetrazol causes polysynaptic responses to appear in the dentate gyrus. Neuroscience. 1995; 68:407–413. [PubMed: 7477951]
20. Nehlig A. Mapping of neuronal networks underlying generalized seizures induced by increasing doses of pentylenetetrazol in the immature and adult rat: A c-Fos immunohistochemical study. Eur J Neurosci. 1998; 10:2094–2106. [PubMed: 9753096]
21. Brevard ME, Kulkarni P, King Ja, Ferris CF. Imaging the neural substrates involved in the genesis of pentylenetetrazol-induced seizures. Epilepsia. 2006; 47:745–754. [PubMed: 16650141]
22. Dragunow M, Faull R. The use of c-fos as a metabolic marker in neuronal pathway tracing. J Neurosci Methods. 1989; doi: 10.1016/0165-0270(89)90150-7
23. Mirski MA, Ann L, Terry JB, Fisher RS. Anticonvulsant effect of anterior thalamic high frequency electrical stimulation in the rat Anticonvulsant effect of anterior thalamic high frequency electrical stimulation in the rat. 1997; 28:89–100.
24. Hamani C, et al. Bilateral anterior thalamic nucleus lesions and high-frequency stimulation are protective against pilocarpine-induced seizures and status epilepticus. Neurosurgery. 2004; 54:191–197. [PubMed: 14683557]
25. Fisher R, et al. Electrical stimulation of the anterior nucleus of thalamus for treatment of refractory epilepsy. Epilepsia. 2010; 51:899–908. [PubMed: 20331461]
26. Graves NM, Fisher RS. Neurostimulation for epilepsy, including a pilot study of anterior nucleus stimulation. Clin Neurosurg. 2005; 52:127–134. [PubMed: 16626064]
27. Lee KJ, Shon YM, Cho CB. Long-term outcome of anterior thalamic nucleus stimulation for intractable epilepsy. Stereotact Funct Neurosurg. 2012; 90:379–385. [PubMed: 22922474]
28. McIntyre CC, Savasta M, Kerkerian-Le Goff L, Vitek JL. Uncovering the mechanism(s) of action of deep brain stimulation: activation, inhibition, or both. Clin Neurophysiol. 2004; 115:1239–1248. [PubMed: 15134690]
29. Takebayashi S, Hashizume K, Tanaka T, Hodozuka A. The effect of electrical stimulation and lesioning of the anterior thalamic nucleus on kainic acid-induced focal cortical seizure status in rats. Epilepsia. 2007; 48:348–358. [PubMed: 17295630]
30. Bittencourt S, et al. Microinjection of GABAergic agents into the anterior nucleus of the thalamus modulates pilocarpine-induced seizures and status epilepticus. Seizure. 2010; 19:242–246. [PubMed: 20347349]
31. McIntyre CC, Grill WM, Sherman DL, Thakor NV. Cellular Effects of Deep Brain Stimulation: Model-Based Analysis of Activation and Inhibition Cellular Effects of Deep Brain Stimulation: Model-Based Analysis of Activation and Inhibition. J Neurophysiol. 2004; 91:1457–1469. [PubMed: 14668299]
32. Gonzalo-Ruiz A, Morte L, Lieberman AR. Evidence for collateral projections to the retrosplenial granular cortex and thalamic reticular nucleus from glutamate and/or aspartate containing neurons of the anterior thalamic nuclei in the rat. Exp Brain Res. 1997; 116:63–72. [PubMed: 9305815]

33. Berglind F, et al. Optogenetic inhibition of chemically induced hypersynchronized bursting in mice. Neurobiol Dis. 2014; 65:133–41. [PubMed: 24491965]
34. Krook-Magnuson E, et al. In vivo evaluation of the dentate gate theory in epilepsy. J Physiol. 2015; 10 n/a–n/a.
35. Kasof GM, et al. Kainic Acid-Induced Neuronal Death Is Associated with DNA Damage and a Unique Immediate-Early Gene Response in c-fos-lacZ Transgenic Rats. J Neurosci. 1995; 15:4238–49. [PubMed: 7790908]
36. Goldberg EM, Coulter DA. Mechanisms of epileptogenesis: a convergence on neural circuit dysfunction. Nat Rev Neurosci. 2013; 14:337–49. [PubMed: 23595016]
37. Weitz AJ, et al. Optogenetic fMRI reveals distinct, frequency-dependent networks recruited by dorsal and intermediate hippocampus stimulations. Neuroimage. 2015; 107:229–241. [PubMed: 25462689]
38. Tung JK, Berglund K, Gutekunst CA, Hochgeschwender U, Gross RE. Bioluminescence imaging in live cells and animals. Neurophotonics. 2016; 3:025001. [PubMed: 27226972]
39. Kätzel D, Nicholson E, Schorge S, Walker MC, Kullmann DM. Chemical–genetic attenuation of focal neocortical seizures. Nat Commun. 2014; 5
40. Wicker E, Forcelli PA. Chemogenetic silencing of the midline and intralaminar thalamus blocks amygdala-kindled seizures. Exp Neurol. 2016; 283:404–412. [PubMed: 27404844]
41. Teranishi K, Shimomura O. Solubilizing Coelenterazine in Water with Hydroxypropyl cyclodextrin. Biosci Biotech Biochem. 1997; 61:1219–1220.
42. Rolston JD, Gross RE, Potter SM. A low-cost multielectrode system for data acquisition enabling real-time closed-loop processing with rapid recovery from stimulation artifacts. Front Neuroeng. 2009; 2:12. [PubMed: 19668698]
43. HB, Andrews P, JEK, SM, PPM. Chronux: a platform for analyzing neural signals. J Neurosci Methods. 2010; 192:146–51. [PubMed: 20637804]
44. Quiroga RQ, Kreuz T, Grassberger P. Event synchronization: A simple and fast method to measure synchronicity and time delay patterns. Phys Rev E - Stat Nonlinear, Soft Matter Phys. 2002; 66:1–9.

Highlights

- Inhibitory luminopsins are able to both acutely suppress and delay epileptic discharges in the rat hippocampus.
- Simultaneous inhibition of the dentate gyrus and anterior nucleus of the thalamus was more effective at suppressing behavioral seizures than inhibition of either structure alone.
- Luminopsins offer a non-invasive means for cell-type specific optogenetic manipulation of network-wide activity.

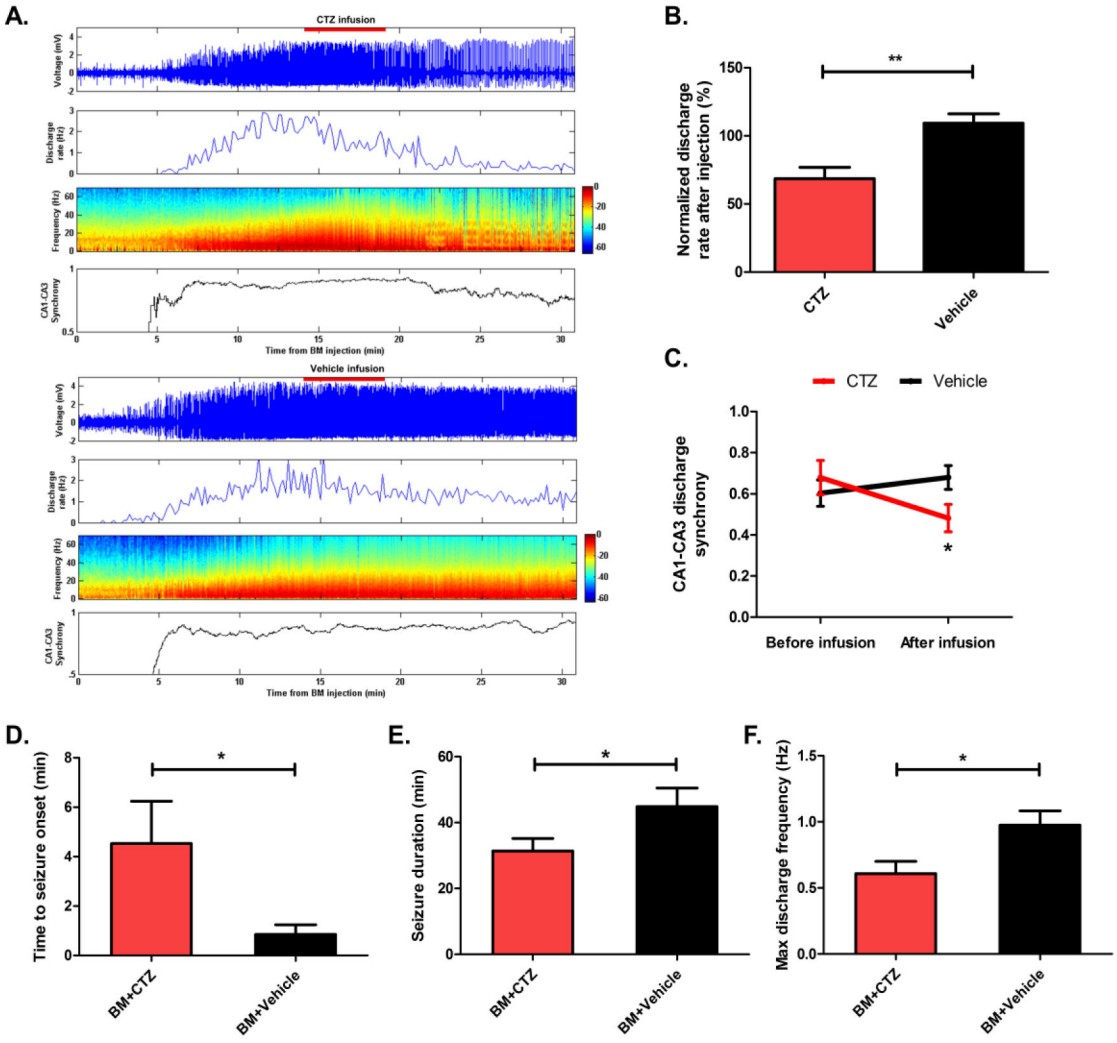

Figure 1. iLMO2 can acutely suppress and delay the development of bicuculline-induced discharges

(A) Top: Representative CTZ injection trial demonstrating acute suppression of bicuculline-induced discharge firing rate, power, and CA1–CA3 synchrony. **Bottom:** Representative vehicle injection trial showing no effects on bicuculline-induced discharges. **(B)** CTZ was able to significantly reduce the discharge rate compared to vehicle (**$p < 0.01$, $n = 8$ trials per group, Student's t-test). **(C)** CTZ was able to significantly reduce the synchrony of discharges in CA1 and CA3 compared to vehicle (*$p < 0.05$, $n = 8$ trials per group, Student's t-test). **(D)** The time to seizure onset was significantly increased when bicuculline (BM) was mixed with CTZ compared to vehicle (*$p < 0.05$, n=5 trials per group, Student's t-test). The seizure duration **(E)** and maximum discharge frequency **(F)** was significantly reduced when bicuculline was mixed with CTZ compared to vehicle (*$p < 0.05$, n=5 trials per group, Student's t-test). Error bars indicate SEM.

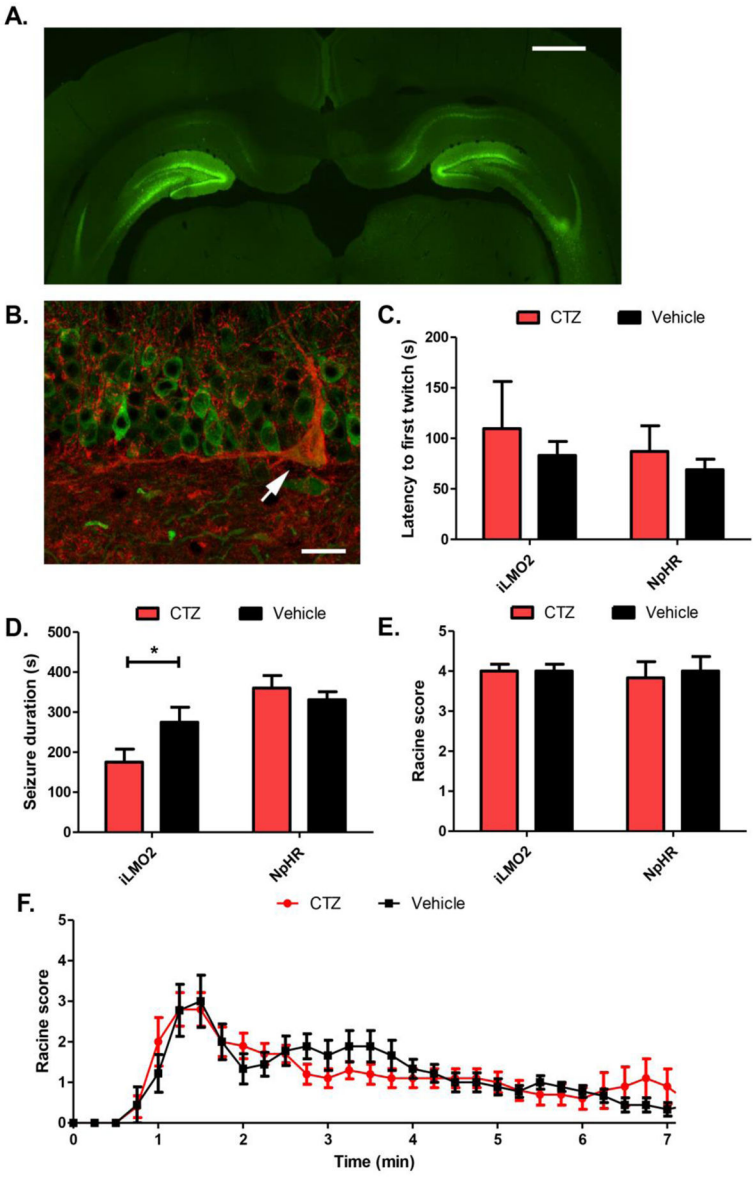

Figure 2. Optogenetic inhibition of the DG with iLMO2 decreases seizure duration

(A) iLMO2 (green) was expressed bilaterally in the DG of the hippocampus. Scale bar: 1 mm. **(B)** iLMO2 does not co-localize with GAD67 (red), indicating that its expression is restricted from GABAergic cells and limited to the granule cells. Arrow: GAD67+ cell with no iLMO2 expression. Scale bar: 10μm. The latency to first twitch **(C)** or seizure severity **(E)** was not significantly increased or decreased, respectively, by CTZ compared to vehicle while seizure duration **(D)** was significantly reduced (*p<0.05, n=10 animals per treatment, Student's t-test). CTZ had no effect in halorhodopsin (NpHR) expressing control animals. **(F)** Mean Racine scores over time after PTZ injection. Error bars indicate SEM.

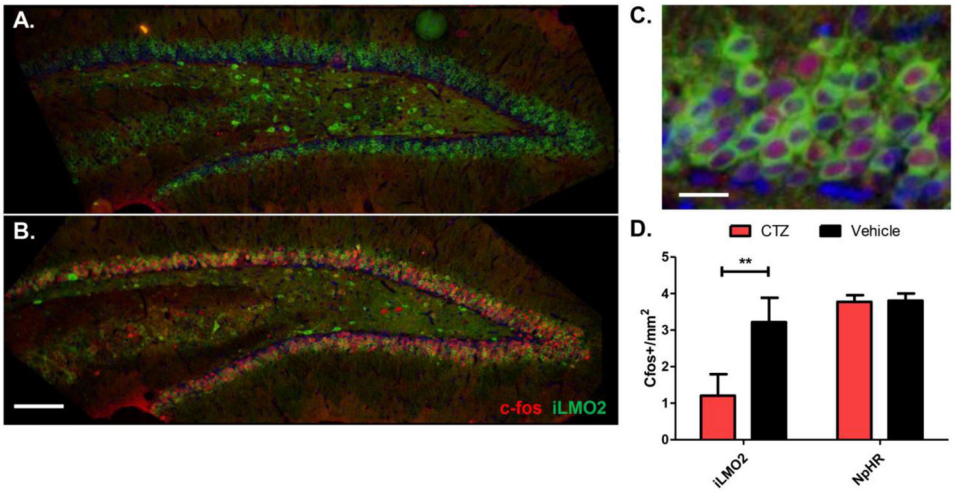

Figure 3. C-fos expression in the DG is reduced in animals treated with CTZ

c-fos expression (red) after CTZ treatment **(A)** is reduced compared to vehicle-treated animals **(B)** Scale bar: 100μm. **(C)** c-fos expression in vehicle treated animals co-localizes with iLMO2 expression (green). Blue: DAPI. Scale bar: 10μm. **(D)** CTZ treated animals have significantly reduced levels of c-fos in the DG on average compared to vehicle treated animals (*p<0.01, n=12 images per group, Mann-Whitney test). CTZ had no effect in halorhodopsin expressing control animals. Error bars indicate SEM.

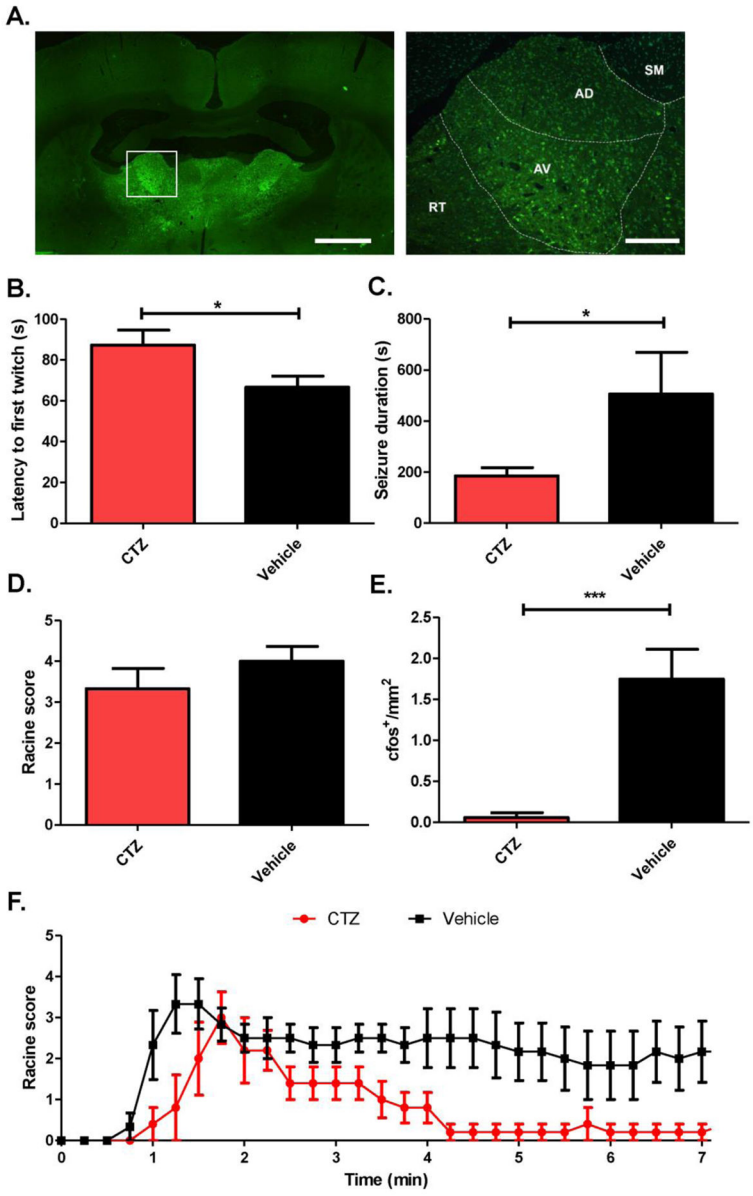

Figure 4. Optogenetic inhibition of the ANT with iLMO2 decreases seizure duration and onset

A. iLMO2 (green) is expressed bilaterally in glutamatergic neurons of the ANT (left, scale bar: 1mm). Right: higher magnification of boxed area showing subnuclei of the ANT (AD: anterodorsal and AV: anteroventral nuclei) and surrounding nuclei (SM = stria medularis, RT = reticular nucleus). Scale bar: 100μm. CTZ significantly increased (*p<0.05, CTZ group n=4 animals, vehicle group n=6 animals, Student's t-test) the latency to first twitch **(B),** and significantly reduced (*p<0.05, n=5 animals per group, Student's t-test) the seizure duration **(C).** CTZ did not significantly affect the seizure severity **(D),** but was able to significantly reduce the amount of c-fos in the DG (p<0.001, n=16 images per group, Mann-Whitney test) **(E). (F)** Mean Racine scores over time after PTZ administration. Error bars indicate SEM.

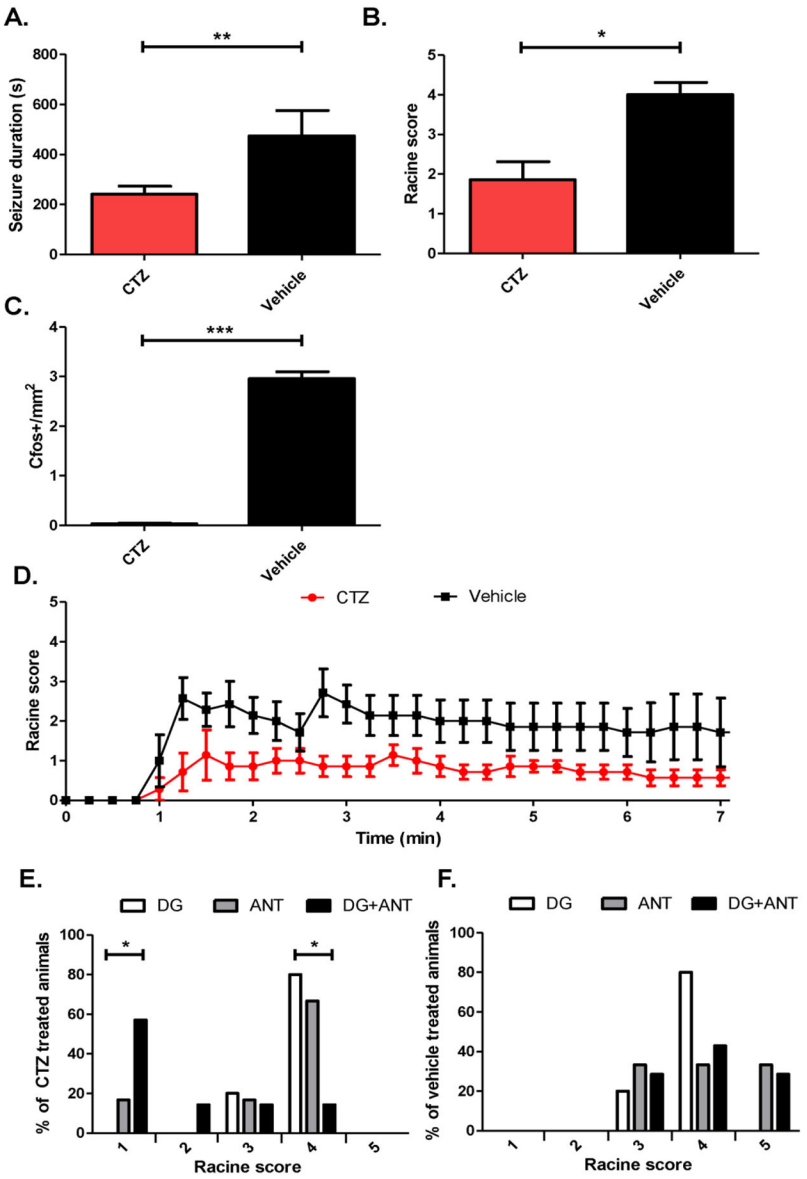

Figure 5. Simultaneous optogenetic inhibition of the DG and ANT reduces overall seizure severity and duration

CTZ significantly decreased seizure duration (*p<0.01, CTZ group n=5 animals, vehicle group n=4 animals, Student's t-test) **(A),** significantly decreased (*p<0.05, n=6 pairs, Wilcoxin matched pairs test) seizure severity **(B)**, and significantly decreased (*p<0.0001, n=19 images for CTZ group, n=16 images for vehicle group, Mann-Whitney test) the amount of c-fos in the DG **(C)** compared to vehicle. **(D)** Mean Racine scores over time after PTZ administration. **(E)** Percentage of CTZ treated animals for each Racine level. There was a significantly higher percentage of animals with Racine level 1 seizures in animals expressing iLMO2 in the DG+ANT compared to DG alone (*p<0.05, n=10 animals for DG group, n=7 animals for DG+ANT group, Fisher's exact test). In addition, there was a significantly lower percentage of animals with Racine level 4 seizures in animals expressing iLMO2 in the DG+ANT compared to DG alone (*p<0.05, n=10 animals for DG group, n=7

animals for DG+ANT group, Fisher's exact test). **(F)** There was no significant difference in the percentage of animals for each Racine level among the different groups that were treated with vehicle. Error bars indicate SEM.